

## Further Studies of the Interaction of Hydrogen with Graphite Nanofibers

C. Park, P. E. Anderson, A. Chambers, C. D. Tan, R. Hidalgo, and N. M. Rodriguez\*

Department of Chemistry, Hurtig Hall, Northeastern University, Boston, Massachusetts 02115

Received: February 9, 1999; In Final Form: September 22, 1999

Catalytically grown graphite nanofibers (GNF) are molecularly engineered structures that are produced by the interaction of carbon-containing gases with small metal particles at temperatures around 600 °C. The fibrous solids consist of minuscule graphene sheets stacked at various angles with respect to the fiber axis. This arrangement generates a material possessing unique chemical properties because unlike conventional graphite crystals, only edges are exposed. Such a conformation produces a material composed entirely of nanopores that can accommodate small-sized adsorbate molecules, such as hydrogen, in the most efficient manner. In addition, the nonrigid pore walls can expand to accommodate the gas in a multilayer conformation. GNF exhibit extraordinary behavior toward the sorption and retention of hydrogen at high pressures and abnormally high temperatures. In this paper we discuss some of the critical factors involved in the adsorption of molecular hydrogen and the influence that this process exerts on the structural characteristics of the material. In addition, the deleterious effect of water vapor on the performance of the GNF is highlighted.

### Introduction

The ever-growing demand for energy and the increase in environmental pollution concerns are exerting pressure for the development of cleaner fuels and more efficient processes. The conventional internal combustion process produces an array of pollutants including particulate materials, nitrogen oxides, sulfur oxides, hydrocarbons, carbon monoxide, as well as large amounts of carbon dioxide.<sup>1</sup> A new technology that is becoming the subject of increasing research effort is that of fuel cells.<sup>2</sup> Hydrogen, the energy source in these systems, is dissociated with the aid of a catalyst to generate two protons and two electrons. After diffusion through a membrane, the protons react with oxygen over a catalyst to produce water. Since in this reaction direct conversion from chemical into electrical energy is realized, the efficiency of the operation is nearly 3 times that achieved with the thermal generated processes. The overwhelming advantage of hydrogen as an energy source lies in the fact that in addition to being one of the most abundant found in nature, it can easily be regenerated, therefore constituting a true renewable energy source. Unfortunately, owing to the lack of a suitable storage system and a combination of both volume and weight limitations, the use of this technology has been restricted in mobile applications.

Graphite is a layered solid in which the various planes are bonded by van der Waals forces where the minimum distance possible between the carbon layers for single-crystal graphite is 0.335 nm. In this crystalline structure, delocalized  $\pi$  electrons form a cloud above and below the basal plane, and it is this arrangement that imparts a certain degree of metallic character to the solid that results in a relatively high electrical conductivity across each carbon layer. The interlayer spacing in graphitic materials is a property dependent on a number of parameters, including the nature and the thermal history of the precursor, and can vary between 0.335 and 0.342 nm, which by appropriate intercalation procedures can be expanded to values of 0.9 nm.<sup>3,4</sup> Unfortunately, in its conventional form, graphite has an extremely low surface area (about 0.5 m<sup>2</sup>/g), and this aspect

has tended to limit its usefulness as a practical selective adsorption agent.

In the current investigation we have successfully overcome the shortcomings of conventional graphite as a storage medium for hydrogen by using graphite nanofibers (GNF). These solids are the product of the decomposition of certain hydrocarbons over selected metal particles.<sup>5,6</sup> The material consists of graphene sheets, the orientation of which can be controlled by the choice of the catalyst used in the preparation procedure. Thus, by manipulation of various parameters, it is possible to produce an array of structures ranging from "tubular" to "ribbonlike" arrangements. These fibrous structures possess a small cross-sectional area, which is estimated to be on average 50 nm<sup>2</sup>, combined with an abundance of exposed edges.<sup>7</sup> These types of materials combine the structural architecture of graphite with a relatively high external nitrogen surface area of about 250 m<sup>2</sup>/g.

A further factor to be taken into consideration is the functionality of the graphite nanofiber surface. Graphitic materials in their pristine state and free of surface oxygen groups are hydrophobic in nature. Following normal activation procedures such materials exhibit a certain degree of hydrophilic character. Under these circumstances, the interaction of graphite with water molecules can be greatly enhanced because of the presence of various oxygenated groups (peroxide, ether, keto, or aldehyde) that are neither acidic nor basic in nature but can impart polarity to the structure.<sup>8</sup> The distribution of polar groups in active carbon is random, whereas in graphitic materials such as GNF, such sites are always located at the edges of the graphene sheets constituting the crystalline structure. It has been demonstrated that following treatment in an oxygen plasma, acidic groups were introduced onto the graphite surface, while nitrogen and ammonia plasmas generated basic functionalities.<sup>9–11</sup> The possibility of controlling the acid–base properties of the GNF could have a direct impact on the adsorption characteristics of these materials.

In an earlier publication we reported that when samples of certain types of graphite nanofiber were placed in a high-pressure adsorption unit, hydrogen uptake to unprecedented

\* To whom correspondence should be addressed.

levels was obtained at room temperature under conditions that would not have been considered possible in more traditional adsorbent materials.<sup>12</sup> Evidently, values achieved for sorption of hydrogen in nanostructures were over an order of magnitude higher than those found with conventional hydrogen storage materials such as metal hydrides.<sup>13–19</sup>

The extraordinary hydrogen adsorption behavior exhibited by GNF is believed to be due to the unique structure adopted by these molecularly designed solids, which consist of an infinite number of diminutive graphite layers stacked at particular angles with respect to the fiber axis. The interlayer spacing produces an arrangement of nanopores, and since in this unique material only graphite edges are exposed, the solid exhibits the highest ratio of nanopore volume to total volume. The low packing density combined with the relative stiffness of these structures has led us to the assumption that there is no generation of macropores within the void space of the fibers. Under such circumstances, all of the adsorption surface is confined to the slit-shaped pores. Since hydrogen possesses a kinetic diameter of 0.289 nm, a value slightly smaller than that of the interlayer spacings in graphite, adsorption occurs through a mechanism involving the diffusion of gas molecules into the inner regions of the solid. Another aspect of significance in this regard is that since the individual graphite platelets are held together by van der Waal forces and not by chemical bonds, the walls of these nanopores can readily undergo expansion to accommodate hydrogen in a multilayer conformation. Such an arrangement of short nanosized pores was indeed found to be capable of accommodating extremely large amounts of hydrogen.

When hydrogen adsorption experiments were carried out at  $-196\text{ }^{\circ}\text{C}$  and pressures up to 1 atm, it was found that the volume sorbed was only about one-fifth of that obtained with active carbon under the same conditions. At room temperature, however, the volume of hydrogen absorbed on GNF was about twice that of the active carbon.<sup>20</sup> These findings have spurred a great deal of interest in the scientific community, and a number of groups have started to work in this area.<sup>21,22</sup> In a recent publication by Chen and co-workers<sup>22</sup> it was reported that when catalytically grown carbon nanostructures that had been doped with alkali metals were subsequently exposed to hydrogen, an increase of up to 20% in the weight of the sample was observed.

The interaction of hydrogen with carbon nanostructures has also been the subject of tremendous interest from the point of view of modeling studies following the earlier disclosures of abnormally high hydrogen uptake in single-walled carbon nanotubes (SWNT)<sup>23</sup> and certain types of graphite nanofibers.<sup>12</sup> Using a phenomenological interaction potential, Stan and Cole<sup>24</sup> examined the adsorption of hydrogen in carbon nanotubes. They concluded that the adsorption potential was not sufficient to account for the discrepancies encountered between the calculated heat of adsorption and the data reported by Dillon and co-workers.<sup>23</sup> Darkrim and Levesque<sup>25</sup> calculated hydrogen adsorption capacities of SWNT with diameters ranging from 0.7 to 1.96 nm and concluded that a diameter of 1.174 nm and an intertube spacing of 0.7 nm gave the highest storage density. A comparison of the hydrogen uptake by SWNTs and slit-shaped pores was conducted by Rzepka and co-workers<sup>26</sup> who claimed that the optimum geometry for hydrogen storage was attained with a pore size of 0.7 nm. Modeling of the interaction of hydrogen with nanotubes and other materials has also been the subject of research by Wang and Johnson.<sup>27</sup> In general terms it can be concluded from these studies that the slit-shaped geometry is much more favorable for hydrogen uptake than that encountered in the tubelike morphology; however, these predic-

tions indicate that carbon nanotubes will not achieve the storage level required for vehicular transportation application.

The structure of chemisorbed hydrogen on single-crystal graphite has been the subject of both theoretical and experimental investigations.<sup>28–43</sup> Neutron diffraction studies performed by Nielsen and co-workers<sup>28</sup> have demonstrated that at low coverage, the adsorbate adopts a commensurate triangular structure  $\sqrt{3} \times \sqrt{3}$  having a lattice parameter of 0.426 nm, which changes to a more condensed arrangement as the coverage is increased. It was interesting, however, to find that upon formation of a second hydrogen layer, a decrease in the lattice parameter to a value of 0.351 nm was observed. This number is significantly smaller than 0.376 nm, a value corresponding to solid hydrogen at  $-269.3\text{ }^{\circ}\text{C}$ . Evidently the presence of graphite modifies the hydrogen packing characteristics to create a phase that is much more condensed than that of the bulk hexagonal close-packed structure typically present in the solid state.

In the present study, we have attempted to determine various factors that can affect the hydrogen uptake of selected GNF samples and to ascertain the modifications of the structure of the material that accompany the hydrogen adsorption step. In this regard, efforts have been focused on treatments that alter the functionality of the GNF edge sites, since hydrogen access to the interior regions of the material is controlled by the chemical interactions that occur at the surface of the solid. It is shown that the presence of water vapor is one of the major obstacles to achieving optimum hydrogen adsorption by the GNF.

## Experimental Section

Graphite nanofibers were prepared from the decomposition of ethylene, carbon monoxide, and hydrogen mixtures over selected metal powders at temperatures between 500 and 700  $^{\circ}\text{C}$  as described in previous publications.<sup>5,6</sup> The solids were demineralized by immersing them in a mineral acid solution for a period of a week, washed, and dried before testing. GNF samples were examined by high-resolution transmission electron microscopy, temperature-programmed reaction (TPR), thermogravimetric analysis (TGA), X-ray diffraction, and other gas adsorption techniques. For comparison purposes selected experiments were conducted with a powdered sample of activated carbon (American Norit Carbon Co., Inc.). This material had a BET  $\text{N}_2$  surface area of 1000  $\text{m}^2/\text{g}$  and micropore and macropore volumes of 0.36  $\text{cm}^3/\text{g}$  and 0.41  $\text{cm}^3/\text{g}$ , respectively.

Hydrogen adsorption studies were performed in a custom-built unit consisting of a stainless steel sample cell, the volume of which was 120.4  $\text{cm}^3$  (including void space), connected to a 508  $\text{cm}^3$  hydrogen reservoir container via a high-pressure valve. The sample cell is also fitted with an additional inlet, which allows one to perform pretreatments to the solids while avoiding any contact with air prior to exposure of the material to hydrogen. Calibration of the unit was conducted by filling the reservoir tank with hydrogen at pressures in excess of 2000 psi and allowing the system to reach thermal equilibrium. The pressure was constantly monitored to determine the absence of leaks over a minimum period of 6 h. Following this procedure, the sample cell was evacuated via an oil-free pumping system and hydrogen allowed to expand from the reservoir into the entire system. Once again, pressure was monitored for sufficient time to allow for thermal equilibrium to be reached. The ratio of the initial to final pressure gave the constant for the apparatus. In a further set of experiments the protocol described above was followed in the presence of a 0.5 g sample of active carbon, which in turn served as a blank.

Weighed amounts of GNF were loaded into the sample container and subjected to selected pretreatments. Following this procedure, the entire system was evacuated in an oil-free environment for about 5–10 h while the external surface of the vessel was heated at 150 °C. The connecting valves were then closed, the sample cooled to room temperature and maintained in this condition for several hours. Hydrogen was permitted to enter the reservoir vessel and a sufficient amount was allowed for the pressure to reach thermal equilibrium. The connecting valve between the reservoir and the sample cell was then opened, and hydrogen immediately gained access to the sample where adsorption was allowed to proceed at room temperature. The volume occupied by the GNF sample was calculated to be 0.23–0.45 cm<sup>3</sup>, based on a density of 2.20 g/cm<sup>3</sup> (less than 0.03–0.07% of the total volume of the vessel). Adjustments were also made to take into account the departure from ideal gas conditions by using the compressibility factor of hydrogen, 1.05, at the working pressure.

In a typical experiment, the sample vessel of the adsorption unit was filled with 0.5–1 g of loosely packed GNF and the system allowed to interact with hydrogen at pressures in excess of 1600 psi at room temperature. The amount of sample used was limited by the low packing density brought about by the physical nature of the material. Changes in pressure were carefully monitored as a function of time for a period of at least 24 h. It was established that after an initial rise, the temperature reached equilibrium after a period of 3.5 h.

At the completion of the adsorption cycle, hydrogen was allowed to slowly exit the system through a regulating valve and the volume of hydrogen determined by displacement of water. The volume of hydrogen desorbed at room temperature was compared with that obtained from the same vessel under identical pressure in the absence of a GNF sample. Temperature and atmospheric pressure were carefully monitored during this step. The difference between these two values gave the amount of recovered hydrogen from the GNF sample. In some investigations this protocol was repeated for a number of cycles in order to establish the integrity of the material under such a sequence of treatments.

Throughout these processes the adsorption unit was continuously monitored with a high-sensitivity hydrogen detector (Laboratory Safety Supply, Wisconsin) to ensure a complete absence of leaks in the system. The unit was regularly checked for internal leaks; this was accomplished by pressurizing the equipment with hydrogen in the absence of any adsorbent and determining the pressure drop. The leak rate was found to be less than 1.0 psi over a 24 h period at constant temperature.

Characterization studies of the GNF both in the pristine state and immediately after high-pressure treatment and decompression from a hydrogen atmosphere were conducted by a variety of techniques. The structural details of the material produced from various preparative procedures were determined by high-resolution transmission electron microscopy using a JEOL 2000 EXII TEM (resolution of 0.18 nm). Suitable transmission specimens were prepared by ultrasonic dispersion of the nanofibers in isobutanol for a few seconds, and then a drop of the suspension was introduced onto a carbon support grid. The degree of crystalline perfection was ascertained from a combination of lattice fringe image analysis, selected area electron diffraction, X-ray diffraction analysis, and temperature-programmed oxidation studies. These respective measurements were performed with the TEM instrument mentioned above, a Scintag XDS-2000 diffractometer using Cu K $\alpha$  radiation and a Cahn 2000 microbalance. This latter unit was also used to

compare the weight loss characteristics of GNF samples that had been subjected to high-pressure hydrogen with those of the same pristine materials. The surface areas and pore size distributions were measured by standard procedures using nitrogen at –196 °C with an Omnisorb 100 CX unit.

Temperature-programmed desorption (TPD) analysis was conducted in a custom-built unit operating in the range 20–950 °C. In these experiments approximately 0.3 g of the GNF was placed in a reaction vessel and initially purged in a stream of N<sub>2</sub> at room temperature for 30 min. Following this step the sample was heated in the presence of N<sub>2</sub> at a rate of 10 °C/min, and as the temperature was progressively raised, adsorbed gases were released from the carbon solids and monitored by a TCD detector. The chemical identity of each desorbed gas was determined by mass spectrometry.

The same unit was also used to conduct temperature-programmed reaction (TPR) studies involving adsorption of hydrogen on GNF samples at atmospheric pressure. In this series of experiments, approximately 0.3 g of a GNF sample was initially heated in nitrogen at 950 °C for 30 min in order to remove any adsorbed species from the solid. The system was then cooled to the desired reaction temperature in the presence of the inert reactant. Consecutive pulses of a known volume of hydrogen at atmospheric pressure were then injected into the gas stream using a gas sampling valve and allowed to interact with the GNF sample until no further retention of the reactant gas was detected with the TCD.

## Results and Discussion

**Characterization Studies.** TEM examinations indicated that under specific operating conditions, graphite nanofibers were the exclusive form of solid carbon generated in the reaction, there being no evidence for the accumulation of other less ordered forms of carbon. The typical appearance of the nanofibers can be seen in the transmission electron micrograph in Figure 1. At high resolution, it is possible to observe the existence of the lattice fringe images of the graphene layers that are arranged in a “herringbone” conformation, which is highlighted in Figure 2. Detailed measurements established that the spacing between adjacent layers was about 0.34 nm, a value that is characteristic of pure graphite. It was possible to grow nanofibers that were comprised of graphite sheets arranged in other conformations, such as a “platelet” form in which individual layers were aligned perpendicular to the fiber axis. Subsequent studies, however, established that the “herringbone” structures gave superior performances with respect to hydrogen adsorption capacities. It is evident that the catalytic synthesis of graphite nanostructures, where well-controlled conditions are maintained, produces high-purity materials in which the only impurity is the metal used as the catalytic entity for the synthesis, and such particles can easily be eliminated by treatment in 1 M hydrochloric acid. In our experimental protocol the temperature of the system was always maintained below that of the thermal decomposition of the carbon source in order to prevent the deposition of pyrolytic carbon.

**Heat-Transfer Experiments.** Hydrogen storage experiments were conducted on GNF samples contained in a 6.0 mm thick stainless steel vessel. Following the conventional protocol for gas adsorption experiments, prior to hydrogen exposure, the sample was evacuated while being heated in order to remove gases that might be chemisorbed on the edges of GNF materials. In initial experiments this latter operation was accomplished by wrapping the container in heating tape that was set to various temperatures. Measurements of the respective temperatures on



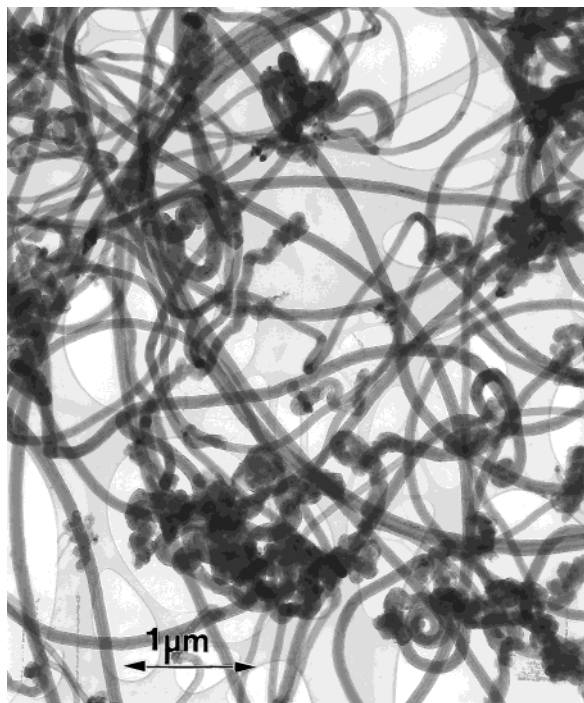


**Figure 1.** Transmission electron micrograph showing the typical appearance of graphite nanofibers produced from the metal-catalyzed decomposition of ethylene/hydrogen mixtures at 600 °C.

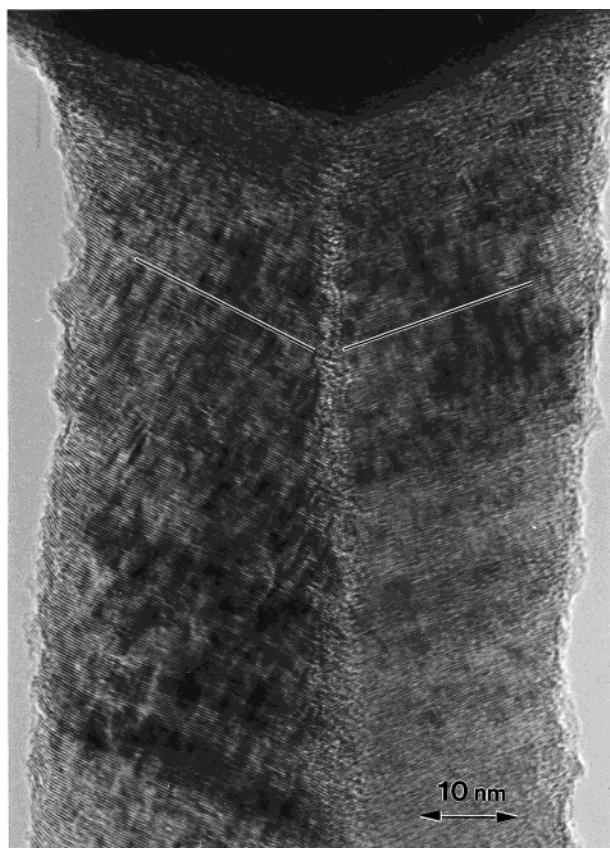


**Figure 2.** High-resolution electron micrograph of a section of a graphite nanofiber showing the lattice fringe images of the graphene sheets within the structure and their "herringbone" arrangement with respect to the fiber axis.

the outside wall of the vessel and inside the GNF bed (Figure 3) indicated the existence of a substantial difference in the values of the two regions. Heat transfer through stainless steel has always been a problem, and it is interesting to find that

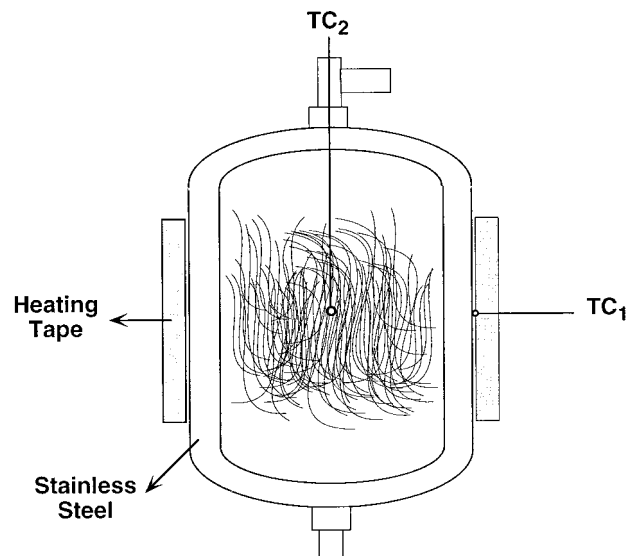


**Figure 3.** Schematic representation of the graphite nanofiber sample contained within the stainless steel adsorption vessel showing the heating arrangement together with the location of thermocouples.

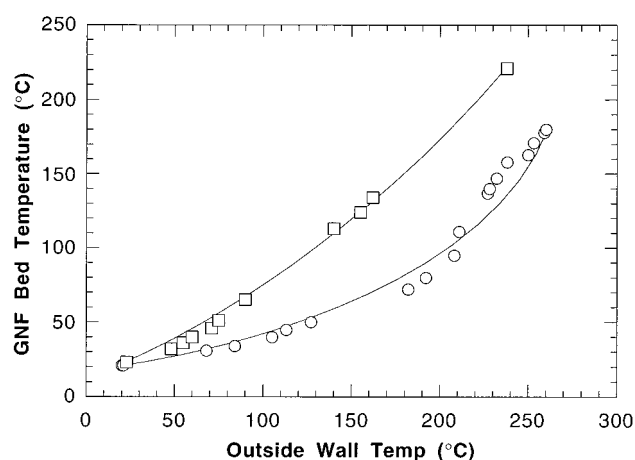


**Figure 4.** Variation in temperature of the GNF bed as a function of the outside wall temperature of the sample vessel: (○) relationship obtained during vacuum conditions; (□) relationship when preheated helium was passed over the sample.

comparable difficulties have also been encountered by other workers during their studies of hydrogen absorption in inter-metallic compounds.<sup>44–46</sup> Figure 4 illustrates the difference existing in the measured temperatures of the outside wall and inside the vessel for a GNF sample treated under vacuum. We believe that this variation is due to the relatively low thermal conductivity of the stainless steel vessel compounded by the lack of physical contact existing in the GNF sample that was loosely packed within the container. Such an arrangement results in a very poor thermal transfer efficiency. If the GNF samples do not reach a sufficiently high temperature during this step, removal of chemisorbed gases such as oxygen and water vapor will be practically impossible. This condition will be manifested by poor hydrogen uptake due to the blocking of edges of the GNF by chemisorbed species.

**Effect of Cycle Experiments on the GNF Hydrogen Absorption/Desorption Characteristics.** In an attempt to improve the thermal transfer efficiency of the current adsorption system, in subsequent experiments the GNF samples, contained in the heated vessel, were flushed with preheated helium. It was found that when this procedure is followed, the ability of GNF samples to sorb hydrogen was substantially improved. This

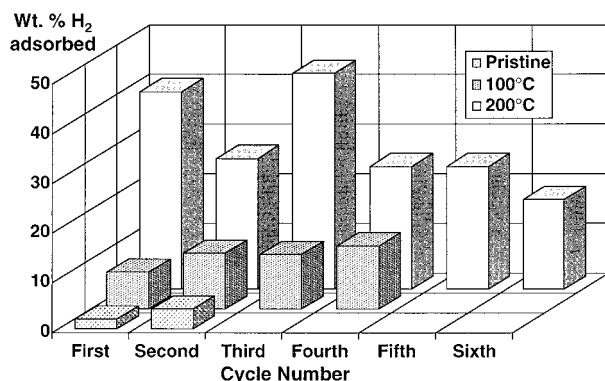


**Figure 5.** Hydrogen adsorption data as a function of the number of adsorption/desorption cycles for samples of GNF taken from the same batch that were in a pristine condition, preheated in situ in an inert gas to 100 °C, and preheated in situ in an inert gas at 200 °C prior to exposure to high-pressure hydrogen. Experimental values reported here were within  $\pm 10\%$ .

pretreatment protocol was used in a further set of experiments designed to investigate the effect of a number of adsorption–desorption cycles on both the structural integrity and performance of the nanofibers. The adsorption data obtained from 0.5 g samples, obtained from the same batch of GNF that had been subjected to a number of cycles following two different pretreatments using preheated inert gas that resulted in the bed being heated at either 100 or 200 °C, are also presented in Figure 5. In all cases the adsorption step was allowed to proceed for a minimum period of 24 h. For comparison purposes we have also included the values obtained for the same batch of untreated nanofibers. Although a modest uptake of about 2 wt % hydrogen was observed for the untreated nanofibers, the adsorption capacity of the material under these conditions is quite low. Duplicate experiments showed that the adsorption data were reproducible to within  $\pm 10\%$  when samples from the same batch of GNF were used.

In a second series of experiments, the nanofibers were initially subjected to the 100 °C pretreatment and it can be seen that a significant improvement in hydrogen adsorption capacity was achieved. When a further sample of the same material was exposed to the 200 °C pretreatment, a much more improved performance was observed. These experiments are an indication of the extremely reactive nature of the edge sites that contain oxygenated groups as revealed by preliminary experiments using XPS. The presence of such groups can lead to cross-linking, a phenomenon that prevents the structures from collapsing when subjected to a mechanical stress. On the other hand, these functional groups can strongly chemisorb water and oxygen molecules and subsequently prevent hydrogen from accessing the internal structure.

In succeeding adsorption experiments, it was apparent that once the nanofibers had reached a level of saturation, unless the adsorbed hydrogen was completely removed, the adsorption capacity achieved in the subsequent cycle was lower. Our current system does not allow us to completely eliminate stored hydrogen at room temperature, and this aspect accounts for the progressive drop in uptakes as a function of cycle number.

In these experiments the sample was only removed from the absorption cell after the final cycle and then a small section was examined using high-resolution TEM. While this procedure was conducted as rapidly as possible following the final desorption step, there was a significant time delay necessitated by the requirement of preparing a suitable specimen for the electron microscopy investigation. Examination of the nanofibers

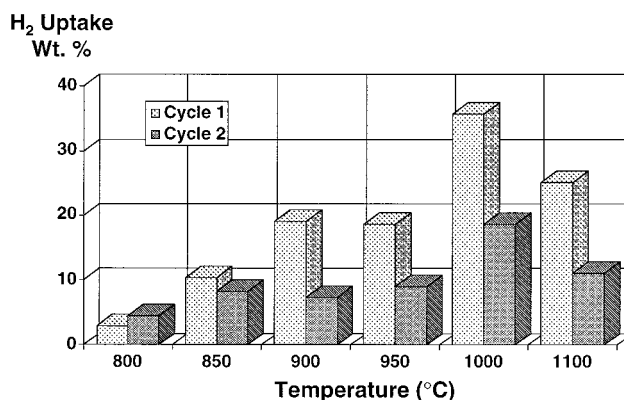


**Figure 6.** Effect of external preheating of similar samples of GNF at various temperatures in an inert gas prior to conducting high-pressure hydrogen adsorption experiments at room temperature. Experimental values reported here were within  $\pm 10\%$ .

that been subjected to this sequence of high-pressure treatments in hydrogen at room temperature failed to reveal any discernible changes in the structural perfection of the material. Caution must be exercised, however, before concluding that the nanofibers maintained their original dimensions throughout these operations, since we cannot dismiss the possibility that fracturing of individual structures occurred, resulting in the generation of smaller entities that still possessed the same initial lattice spacing.

**Pretreatments of Graphite Nanofibers.** When graphite nanofibers that were freshly prepared or that had been kept for several days were placed in the adsorption unit, their performance toward hydrogen storage was rather poor. As with many carbon materials, it was anticipated that humidity, as well as the presence of other chemisorbed gases, could have an effect on the evaluation of their storage properties. Preliminary tests had also indicated that certain of these materials contained some hydrogen, which we believe had been retained during the synthesis. Figure 6 illustrates the effect of pretreatment temperature on the subsequent hydrogen adsorption capacity of GNF. It can be seen that marked improvements in gas adsorption were achieved as the treatment temperature was increased. We believe that the enhancement in the adsorption capacity is due to the removal of chemisorbed species that are strongly adsorbed both at the edges and between the graphene layers in the GNF and that prevent access of hydrogen to the inner regions of the structure. Taking into account that the maximum value was obtained following treatment at 1000 °C, we can speculate that the species that had been removed include certain oxygenated groups that act as centers for the adsorption of oxygen and water molecules.

Miura and Morimoto<sup>47</sup> have studied the interaction of H<sub>2</sub>O with graphite surfaces that have been modified using various treatments. They concluded that heating of the solid in hydrogen at temperatures of about 1000 °C resulted in the replacement of the surface oxide groups by C–H bonds and this modification in chemical functionality was manifested by a change in adsorption properties. This finding is consistent with the data obtained in the current investigation, where the high-temperature treatments performed in an “inert” atmosphere were found to generate GNF samples that exhibited an improved performance with respect to subsequent hydrogen adsorption. It is therefore reasonable to assume that the small amount of hydrogen remaining within the structure of the nanofibers after the preparation procedure is sufficient to reduce the oxygenated groups during the high-temperature treatment. When the nanofi-

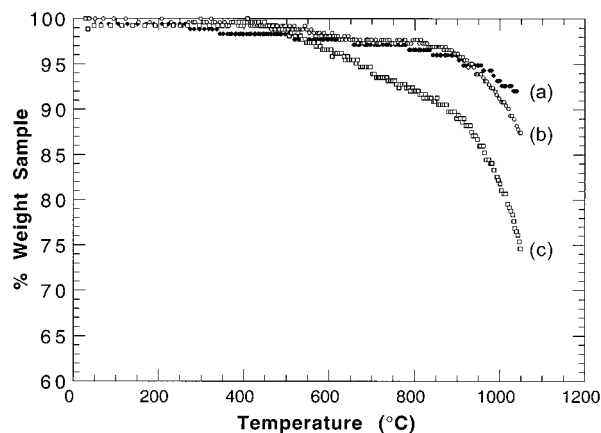


**Figure 7.** Weight loss profiles as a function of temperature for various GNF samples: (a) pristine GNF heated in pure He; (b) pristine GNF heated in 10%  $\text{H}_2/\text{He}$ ; (c) GNF exposed to high-pressure  $\text{H}_2$  for 24 h and then heated in pure He.

bers were treated at even higher temperatures, the modifications in the functionality derived from such treatments appear to decrease their ability to adsorb hydrogen. Although it has not been possible to establish with a any degree of certainty the origin of this behavior, we believe that at some point dangling bonds at the edges of the nanofibers can produce a curling of the structure that ultimately results in the closure of the porosity.

**Thermogravimetric Studies.** Thermogravimetric studies were carried out on demineralized GNF samples in the pristine state and immediately following treatment in hydrogen at high pressures. It should be stressed that these samples were exposed to the atmosphere prior to conducting the TGA analyses, and therefore, some perturbations in the chemical characteristics could have occurred during the transfer operations. Figure 7 illustrates weight loss profiles for various GNF samples as they were thermally treated in a helium atmosphere. It is apparent that the weight change for pristine GNF samples observed in helium and in the presence of a 10% hydrogen/helium stream produced a very small weight loss, about 3% up to 900 °C, which is probably due to the presence of chemisorbed water vapor molecules. A further weight loss is observed in the presence of 10% hydrogen/helium when samples reach 1000 °C, a temperature at which possible removal of oxygenated groups begins to take place leading to a further 5% loss.

A completely different pattern of behavior was observed for the same type of GNF material that had previously been exposed to a high-pressure hydrogen treatment. In this case, when the sample was heated in helium, it started to lose weight at about 550 °C and the rate of this process increased as the temperature was progressively raised to a maximum level of 1050 °C. Although desorption experiments had already been conducted, where a substantial amount of the previously adsorbed hydrogen had been removed, it is evident that some hydrogen still remained in the sample. Inspection of this profile indicates that a net weight loss of 15% was recorded compared to the results of the blank experiment (10%  $\text{H}_2/\text{He}$ ). While the material may also contain some water vapor, we believe that the major fraction of the weight loss can be attributed to the release of the strongly held hydrogen that remained in the carbon structure following the normal desorption protocol.

**Temperature-Programmed Desorption Studies.** In a complementary set of experiments samples of GNF and active carbon were examined by TPD before and after exposure to a high pressure of hydrogen. For comparison purposes we also examined the behavior of a similar sample of GNF that had

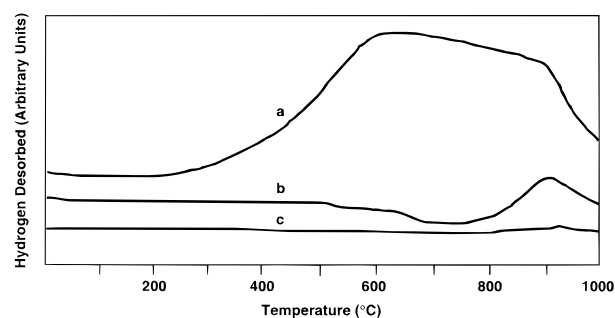


**Figure 8.** Temperature desorption scans of (a) a GNF sample that had been subjected to a high-pressure  $\text{H}_2$  adsorption/desorption cycle; (b) a GNF sample exposed to 1 atm  $\text{H}_2$ ; (c) an active carbon sample treated under conditions identical to those of sample in (a).

been exposed to hydrogen at atmospheric pressure. The typical patterns of behavior that were observed with this technique in the presence of a nitrogen carrier gas are presented in Figure 8. Inspection of these scans shows that nanofibers that have been subjected to a high-pressure hydrogen treatment still contain an appreciable quantity of gas that does not start to desorb until the temperature is raised to about 550 °C. Furthermore, it is necessary to increase the temperature to over 900 °C if one is to achieve complete removal of this component. There is also evidence that retention of gas occurs from the GNF sample treated in low-pressure hydrogen. Subsequent analysis of the gas that was collected from both these samples during this stage of the experiment by mass spectrometry showed it be hydrogen, there being no evidence for the presence of methane, the product that one would associate with hydrogasification of carbon.

It is interesting to compare these patterns of behavior with that obtained when a sample of active carbon that had also been exposed to high-pressure hydrogen was tested under the same conditions. Scrutiny of this scan shows the existence of a trace amount of gas that is released from the sample at about 850 °C. Finally, a sample of active carbon that had not been treated in high-pressure hydrogen was examined by this method. It was evident that the sample did not contain any significant amount of stored gas, since the scan remained relatively smooth over the entire temperature range.

The data obtained from the TGA and TPD experiments furnish a consistent picture with regard to the finding that following a typical high-pressure adsorption/low pressure desorption cycle, the GNF samples still retain significant amounts of stored hydrogen. The existence of two types of adsorbed hydrogen in these structures, one that is relatively easily released and the other that is strongly bound, is a fascinating discovery. It is also significant that this behavior is not displayed by an active carbon sample when subjected to the same set of procedures. It is this difference that points to the participation of the delocalized p electrons that exist on the graphite basal regions of the GNF structures.

Brown and co-workers<sup>40</sup> have used the data of Nielsen and co-workers<sup>28</sup> to calculate the ratio of hydrogen to carbon atoms in the various conformations that have been identified using neutron diffraction scattering experiments.<sup>28</sup> In the  $\sqrt{3} \times \sqrt{3}$  low-coverage commensurate structure, hydrogen molecules are placed over alternate hexagons in the graphite structure and as such would generate a configuration where there is one hydrogen atom for every three carbons, or approximately 2.78 wt %. At higher coverage, the H/C ratio could increase to 1, which would yield 8.33 wt %. Clearly, the results of the present investigation suggest that in our experiments the amount of hydrogen retained



within the GNF surpasses both these structures. Neutron diffraction studies of hydrogen adsorbed on the basal plane of graphite lead to the determination of an adsorbate structure that is more condensed than that observed for the bulk hexagonal close packing of hydrogen molecules. Since in situ X-ray diffraction or neutron scattering experiments have not yet been performed on hydrogen in GNF, it is not possible to state with any degree of certainty what type of condensed structure is generated under the current conditions.

Although modeling studies are extremely useful for the prediction of the behavior of the carbon–hydrogen interaction, there is a great deal of information that is still unknown about these unusual systems. The various models used to explain the interaction of hydrogen with both GNF and SWNT (single-walled nanotubes) make the assumption that a physical interaction exists between the gas and the graphene layers. The discrepancy between the experimental and calculated values is a strong indication that a much more complex situation is operative. The experimental analysis of gaseous products following hydrogen adsorption supports our belief that dissociation of hydrogen does not occur, since no hydrocarbon products were detected. If such a reaction were to take place, the resulting atoms would readily react with the carbon atoms in the graphite lattice and form C–H bonds, resulting in the release of methane or perhaps other hydrocarbon products upon an increase of the temperature. Since no hydrocarbon products were detected following heating of the material in an inert atmosphere at temperatures of up to 1000 °C, we can confidently conclude that the adsorption phenomenon did not involve the participation of hydrogen atoms.

Calculations performed by Rzepka and co-workers<sup>26</sup> indicate that it is only possible to achieve a maximum storage density equivalent to 20% of that of liquid hydrogen at a slit pore distance of 0.7 nm. We have established that following synthesis, GNF contain a substantial amount of hydrogen; however, X-ray diffraction analysis indicated that this event was not accompanied by a substantial expansion of the graphite lattice. These results substantiate our earlier proposition that the size of hydrogen within the confined systems of GNF is much smaller than that used in most calculations. Given the level of hydrogen sorption encountered in these systems, it is possible to speculate that two types of adsorption are occurring. The first type is chemisorption, where some charge complex is formed in which the hydrogen transfers electrons to the graphite lattice, a process that might result in an entity (perhaps positively charged) having a much more reduced size than that assumed in most calculations.<sup>25–27</sup> The second type of adsorption would be physisorption, where the hydrogen molecules are not necessarily in contact with the graphite lattice but surrounded by other hydrogen species. These two types of adsorption have been proposed for hydrogen entering the lattice of graphite intercalation compounds (GIC).<sup>48–52</sup> Physisorption in GIC is observed at temperatures of ~200 K in higher stage alkali metal GIC, where the gas molecules appear to stabilize the formation of a condensed phase in the “galleries of the graphite sheets”. The chemisorption phenomenon of hydrogen in these materials is purported to involve a back-donation of electrons from the alkali metal to the graphene and hydrogen layers, where dissociated hydrogen species are stabilized in the intercalate spaces. In future studies we shall attempt to ascertain the nature of the proposed hydrogen–GNF complex with the aid of neutron diffraction scattering experiments.

**Temperature-Programmed Reaction.** The effect of temperature on the hydrogen sorption capacity of GNF at atmo-

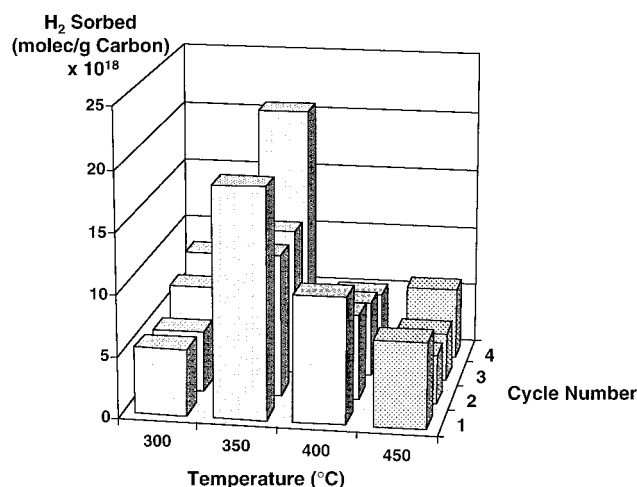


**Figure 9.** Adsorption of hydrogen in a GNF sample at various temperatures and atmospheric pressure as a function of temperature.

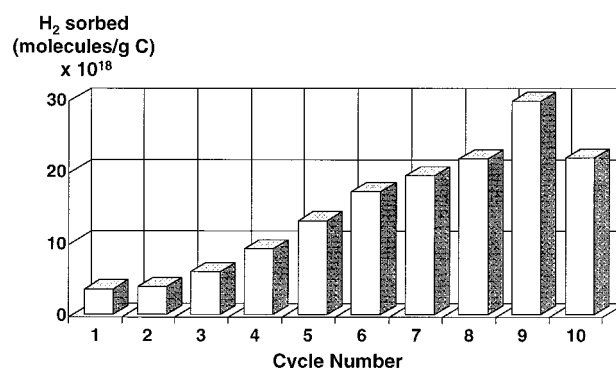


**Figure 10.** Adsorption cycles of hydrogen in a GNF sample at 350 °C and atmospheric pressure.

spheric pressure was determined by temperature-programmed reaction (TPR) experiments. Figure 9 illustrates the behavior of a GNF sample as it was exposed to controlled amounts of pulsed hydrogen until a saturation condition was reached, i.e., until no further retention of hydrogen was observed. At a given temperature the GNF sample was subjected to a total of four cycles, each consisting of several individual pulses. Following this procedure, the solid was treated in nitrogen at 350 °C overnight before proceeding to the next cycle. Retention of the reactant gas by the nanofibers was found to be dependent on a number of factors, including temperature as well as the previous history of the material. From these experiments it was apparent that although a modest uptake was obtained at 300 °C, maximum sorption was achieved when the sample was being heated at 350 °C. At higher temperatures of 400 and 450 °C hydrogen retention by the nanofibers was attenuated. It is possible that at these temperatures, desorption and sorption are simultaneously occurring, resulting in a reduction of the uptake. These experiments appear to indicate that the process is kinetically driven.

In a further study, a similar sample of GNF was exposed to a total of 10 cycles (each consisting of several pulses of hydrogen followed by overnight treatment in flowing nitrogen). All procedures were conducted at 350 °C, and the data obtained from these experiments are given in Figure 10. It was evident that the hydrogen adsorption capacity increased with cycle number, reaching an optimum level after nine runs. We believe that this trend is a reflection of a progressive drying and cleaning of the edges of the material, thereby generating a GNF surface that is more receptive to adsorption of hydrogen. Unfortunately,

owing to safety concerns, it has not been possible to carry out hydrogen adsorption experiments that involve both high-pressure and high-temperature conditions.

**X-ray Diffraction and Pore Size Distribution Measurements.** On the basis of the unexpectedly high retention capacity for hydrogen found in GNF, we speculated that the interlayer spacing between the graphene platelets was being expanded during the adsorption process.<sup>4</sup> In addition, following exposure of GNF to high-pressure hydrogen, we found that the amount of gas collected during the desorption step was smaller than that calculated by changes in pressure during adsorption. It was this discrepancy that led to the postulate that a significant amount of strongly bound hydrogen was still retained within the structure. If indeed hydrogen was still present within the structure, it would be reasonable to expect that such an occurrence would be manifested by an expansion of the interlayer spacing. Although it has not been possible to make in situ measurements of the changes in lattice parameters of the GNF accompanying hydrogen sorption up to this point in time, we have performed pore size distribution as well as X-ray diffraction examinations of the samples following the hydrogen adsorption/desorption experiments in an attempt to ascertain the existence of any modifications exhibited by the structures. Over a period of a few days we established that small amounts of hydrogen were slowly being released from the nanofibers and that this behavior could readily be observed by placing a hydrogen detector over the sample. Preliminary experiments have also indicated that the desorption of "strongly" held hydrogen could be accelerated if the nanofibers were subjected to a burst of microwave radiation. When this operation was carried out in air, the interaction between the released hydrogen and oxygen resulted in spontaneous combustion as a result of the highly exothermic reaction between the two gases.

Pore size distribution (PSD) measurements indicated that following hydrogen adsorption experiments, the solid underwent substantial structural perturbations. Figure 11 illustrates the changes in the pore size distribution of a GNF sample prior to exposure to a high pressure of hydrogen (Figure 11a), immediately following adsorption/desorption experiments (Figure 11b), and after 8 days of exposure to ambient conditions (Figure 11c). Since nitrogen, the gas used for the determination of the pore size distribution, is not expected to be able to gain access to the interlayer spacing in the pristine GNF, the PSD of this sample is merely a measure of the relative smoothness of surface. Following hydrogen adsorption, however, the GNF sample appeared to undergo structural changes, which were subsequently manifested as a broadening of the PSD profile. This modification can be interpreted as being due to an expansion of the lattice spacing generated by the presence of residual hydrogen, which results in a disruption of the original structure to such an extent that a significant fraction of nitrogen gains access to some of these regions.

Indeed, in other experiments when GNF samples that had been subjected to several high-pressure hydrogen adsorption/desorption cycles were subsequently treated in nitrogen, in a further cycle the adsorption of hydrogen was inhibited. In this case one might argue that the presence of residual nitrogen at the pore mouth of the GNF effectively blocked the access route to hydrogen molecules. It is significant that when this "deactivated" sample was given an intermediate treatment in helium, the storage capacity for hydrogen was restored to its initial high level.

X-ray diffraction experiments were conducted on a pristine sample and after the hydrogen treatment and the ensuing

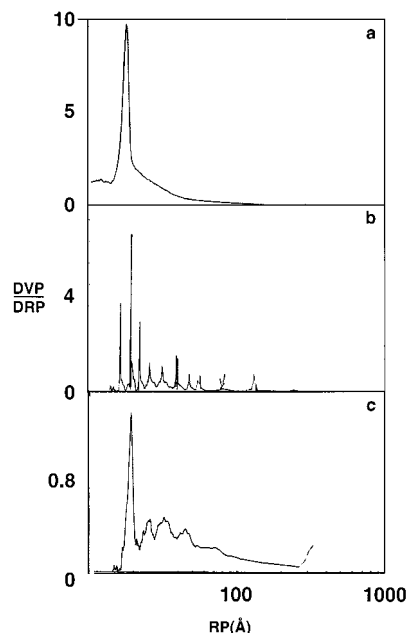


**Figure 11.** Pore size distribution measurements of a GNF sample that had been subjected to a high-pressure hydrogen adsorption/desorption cycle at room temperature: (a) pristine condition; (b) immediately following hydrogen desorption; (c) after a further 8 days at ambient conditions.

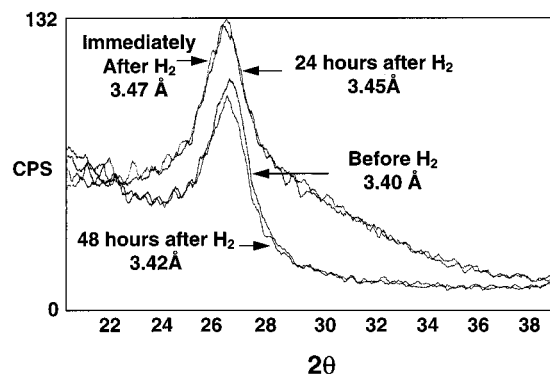


**Figure 12.** Progressive changes in the X-ray diffraction patterns of a pristine GNF sample that was subsequently subjected to high-pressure hydrogen followed by desorption at ambient conditions and after exposure to air for an extended period of time.

desorption step. The different patterns obtained after various periods of time are presented in Figure 12. It is evident that hydrogen induces an expansion of the lattice from 0.340 nm (prior to adsorption) to 0.347 nm following a decrease in the pressure. The structure appears to undergo a relaxation back to the initial value after several hours at ambient conditions.

These changes can be rationalized according to the notion that as hydrogen enters the region between the graphene layers, a concomitant expansion of the lattice takes place to accommodate the gas molecules. Furthermore, we believe that following desorption, sufficient hydrogen still remains within the structure to generate a structure where the layers are separated to a greater extent than that encountered in the pristine state, and that the residual amount of gas is bound in a relatively strong form within the nanofiber structure, being slowly released over a period of time. This process is consistent with the findings that both the pore size distribution and X-ray diffraction patterns gradually relax back to their initial state. Clearly, if the desire is to release all the hydrogen in a single burst, then we must explore the potential of utilizing additional procedures to



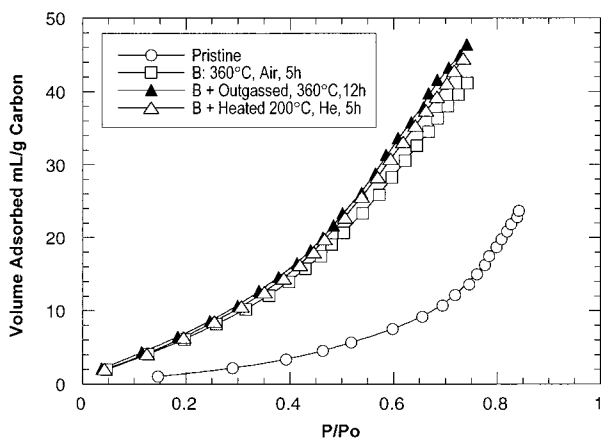


**Figure 13.** Water vapor adsorption isotherms for similar GNF samples that have received different pretreatments.

enhance this step. While raising the temperature is one option, other more sophisticated methods that can be operated at room temperature are being sought.

**Effect of Surface Properties on the Hydrogen Adsorption on GNF.** The lack of reproducibility observed in our preliminary experiments for hydrogen uptake in ostensibly similar samples of GNF has led us to mount a comprehensive program directed at a fundamental understanding of the various parameters that could exert an impact on this process. Because of the unique structure of GNF, which consists entirely of edge regions, the material becomes extremely reactive toward the formation of oxygenated groups at these sites upon exposure to air following the synthesis step. These groups have the ability to transform the chemical nature of the nanofibers from hydrophobic to hydrophilic, and as a consequence, these regions act as centers for the adsorption of water molecules. Since the kinetic diameter of the water molecule, 0.264 nm, is smaller than that of hydrogen, 0.289 nm, diffusion of this adsorbate within the structure of GNF is a more facile process. In addition, the presence of oxygenated groups at edges can also act as adsorption centers for the collection of molecules including oxygen, which will hinder hydrogen migration to the interlayer spaces of the GNF structures.

An example of the interplay between the generation of oxygen functionalities on the nanofiber edge sites and the propensity of the structures to adsorb water vapor molecules can be seen from the adsorption isotherms given in Figure 13. From inspection of these data it is abundantly clear that the GNF materials in the "as grown" state are capable of adsorbing up to 20 cm<sup>3</sup>/g of water at atmospheric conditions. When these nanofibers are given a mild oxidation treatment, sufficient oxygenated groups are generated on the edge sites to make the GNF more hydrophilic in nature. The ramifications of this reaction are manifested in a significant increase in the ability of the GNF to adsorb water, reaching a value of about 50 cm<sup>3</sup>/g. Subsequent outgassing or heating in helium at 200 °C evidently did not remove the oxygen groups; indeed, it was found that there was a slight increase in the capacity of the structures to adsorb water following such a treatment. One may therefore conclude that complete elimination of water from within the graphite structure is virtually impossible once this process has occurred. We have found that careful manipulation and handling of the material are absolutely essential if one is to achieve optimum performance with respect to hydrogen uptake. It should be appreciated that this problem is not exclusive to GNF, since metal hydrides are also vulnerable to the same effects.<sup>13</sup>

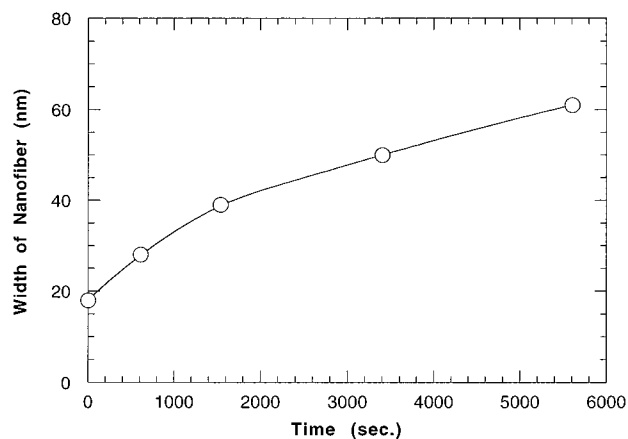


**Figure 14.** Observed increase in width of an individual graphite nanofiber due to the adsorption of water vapor at room temperature as a function of time.

In a complementary series of experiments, controlled atmosphere electron microscopy (CAEM) was used to follow the changes in appearance of samples of GNF during exposure to a helium stream saturated with water vapor at room temperature. The CAEM technique enables one to directly observe the interaction between gases and solids at temperatures over the range 20–1000 °C, and since the data are continuously recorded on a closed-circuit video system, it is possible not only to discern qualitative changes in the appearance of the specimen but also to determine the detailed quantitative kinetics of various events of interest.<sup>53</sup> A detailed analysis of the videotape sequences of these experiments has enabled us to measure the expansion of graphite nanofibers as a function of time during treatment of the sample at room temperature in wet helium over a period of about 2.0 h, and this dependence is presented in Figure 14. Inspection of this plot shows that the width of the nanofibers exhibits an increase of over a factor of 3 during this process, and it was significant to observe that the material retained its structural integrity during this period. Unfortunately, it was not possible to determine the corresponding changes in the longitudinal direction because of the absence of distinguishing features on the body of the nanofibers.

In a further set of experiments the same reactions were carried out with the exception that the specimens were only viewed at the start and termination of the reaction with the electron beam switched off for most of the time. In this way it was possible to establish that the observed expansion of the nanofibers was not due to experimental artifacts created by the effects of electron radiation of the material. Finally, it was interesting to discover that when the gas flow was terminated (and as a consequence, the specimen was exposed to the vacuum conditions prevailing in the microscope), the "expanded nanofibers" did not appear to exhibit any significant degree of shrinkage. This observation would indicate that adsorbed water molecules are held very strongly in this type of material.

While chemisorption of undesirable adsorbates has a profound impact on the subsequent ability of the GNF samples to adsorb hydrogen, it should be stressed that other factors play a key role in the ability to obtain reproducible storage behavior. Examination of GNF samples made under ostensibly identical reaction conditions shows that the product may exhibit subtle differences in structural characteristics and surface conditions. These variations may be attributed to slight changes in the growth temperature, reactant gas flow patterns, and ambient conditions that exist when samples are eventually removed from the reactor. In this regard, we are currently focusing attention

on a number of factors that could be responsible for the observed experimental deviations in batches of GNF grown from the same catalyst systems.

Recent studies by Ye and co-workers have reported on the "high" hydrogen adsorption capacity of SWNT.<sup>54</sup> These workers used sonication methods to "slice open" the structures, presumably in an attempt to accelerate the diffusion of hydrogen into the material. While such a procedure seems plausible, a 10 h treatment under these conditions can cause catastrophic damage, since the potential for rupture of these conformations is quite high. If such structures were to be cleaved across the tube, then there is an equal probability of fracture in the direction parallel to the tube axis. The net result of such a drastic treatment is the indiscriminate explosive opening of the material. In addition, since the  $sp^2$  carbons do not exist in the free state, undesirable functionality can be introduced at the newly formed edges of the flakes. Carbon materials and particularly the edges of graphite are extremely sensitive to the nature of the environment, and as a consequence, these regions will acquire functionality, mainly oxygenated groups unless special precautions are taken to avoid interaction with air.

The extraordinary capacity of GNF to adsorb and retain hydrogen in quantities much higher than those achieved with any other material has tremendous ramifications for portable energy devices. If indeed large-scale production and reproducible performance of the material are realized, then these materials would allow one to transport hydrogen in a much more efficient manner.

## Conclusions

It has been established that careful pretreatment of GNF samples is a critical procedure in order to remove chemisorbed gases from edge and step regions of the structures. Failure to achieve this condition results in a dramatic decline in the performance of the materials to subsequently adsorb hydrogen. It was found that merely heating the vessel containing the GNF adsorbent under vacuum conditions did not appear to remove the adsorbed impurities, and as a consequence, subsequent hydrogen adsorption experiments were unsuccessful. We have demonstrated that structural perturbations to the material were produced following hydrogen sorption experiments and that these features were manifested by expansion of the lattice as indicated by X-ray diffraction experiments and pore size distribution analysis.

**Acknowledgment.** Financial support was provided by the United States Department of Energy, Grant DE-FC36-97GO-10235, and Catalytic Materials Ltd.

## References and Notes

- (1) Taylor, K. C. In *Automobile Catalytic Converters*; Springer-Verlag: New York, 1984; p 120.
- (2) Appleby, A. J.; Foulkes, F. R. *Fuel Cell Handbook*; Van Nostrand: New York, 1989.
- (3) Dresselhaus, M. S.; Dresselhaus, G.; Suguhara, K.; Spain, I. L.; Goldberg, H. A. *Graphite Fibers and Filaments*; Springer-Verlag: Berlin, 1993.
- (4) Dresselhaus, M. S.; Dresselhaus, G. *Adv. Phys.* **1981**, *30*, 139.
- (5) Kim, M. S.; Rodriguez, N. M.; Baker, R. T. K. *J. Catal.* **1991**, *131*, 60.
- (6) Rodriguez, N. M. *J. Mater. Res.* **1993**, *8*, 3233.
- (7) Rodriguez, N. M.; Chambers, A.; Baker, R. T. K. *Langmuir* **1995**, *11*, 3862.
- (8) Groszcek, A. J. *Carbon* **1987**, *25*, 635.
- (9) Sugiura, M.; Esumi, K.; Meguro, K.; Honda, H. *Bull. Chem. Soc. Jpn.* **1985**, *58*, 2638.
- (10) Esumi, K.; Sugiura, M.; Mori, T.; Meguro, K.; Honda, H. *Colloid Surf.* **1986**, *19*, 331.
- (11) Esumi, K.; Kimura, Y.; Nayada, T.; Meguro, K.; Honda, H. *Carbon* **1989**, *27*, 301.
- (12) Chambers, A.; Park, C.; Baker, R. T. K.; Rodriguez, N. M. *J. Phys. Chem. B* **1998**, *102*, 4253.
- (13) Sandrock, G.; Suda, S.; Schlapbach, L. Hydrogen in Intermetallic Compounds. *Top. Appl. Phys.* **1992**, *67*, 197.
- (14) Maeland, A. J. In *Hydrides for Energy Storage*; Andressen, A. F., Maeland, A. J., Eds.; Pergamon: Oxford, 1978; p 447.
- (15) Shilov, A. L.; Padurets, L. N.; Kost, M. E. *Russ. J. Phys. Chem.* **1985**, *58*, 8, 1103.
- (16) Bambakidis, G.; Bowman, R. C., Jr. *Hydrogen in Disordered and Amorphous Solids*; Plenum: New York, 1986.
- (17) Maeland, A. J. In *Metal Hydrides*; Bambakidis, G., Ed.; Plenum: New York, 1981; p 177.
- (18) Suzuki, K. *J. Less-Common Met.* **1983**, *89*, 183.
- (19) Bowman, R. C., Jr. In *Hydrogen Storage Materials*; Barnes, R. G., Ed.; Materials Science Forum; Trans Tech Publications: Aedermannsdorf, Switzerland, 1988.
- (20) Rodriguez, N. M.; Baker, R. T. K. U.S. Patent 5,653,951, August 1997.
- (21) Nützenadel, C.; Züttel, A.; Chartouni, D.; Schlapbach, L. *Electrochem. Solid-State Lett.* **1999**, *2*, 30.
- (22) Chen, P.; Wu, X.; Lin, J.; Tan, K. L. *Science* **1999**, *285*, 91.
- (23) Dillon, A. C.; Jones, K. M.; Bekkedahl, T. A.; Kinag, C. H.; Bethune, D. S.; Heben, M. J. *Nature* **1997**, *386*, 377.
- (24) Stan, G.; Cole, M. W. *J. Low Temp. Phys.* **1998**, *110*, 539.
- (25) Darkrim, F.; Levesque, D. *J. Chem. Phys.* **1998**, *109*, 4981.
- (26) Rzepka, M.; Lamp, P.; de la Casal-Lillo, M. A. *J. Phys. Chem. B* **1998**, *102*, 10894.
- (27) Wang, Q.; Johnson, J. K. *Mol. Phys.* **1998**, *95*, 299; *J. Chem. Phys.* **1999**, *110*, 577; *J. Phys. Chem. B* **1999**, *103*, 4809.
- (28) Nielsen, M. In *Phase Transitions in Surface Films*; Dash, J. G., Ruvalds, J., Eds.; Plenum Press: New York, 1980.
- (29) Freimuth, H.; Wiechert, H. *Surf. Sci.* **1985**, *162*, 432; **1986**, *178*, 716.
- (30) Freimuth, H.; Wiechert, H.; Lauter, H. J. *Surf. Sci.* **1987**, *189*, 548.
- (31) Novaco, A. D. *Phys. Rev. Lett.* **1988**, *60*, 2058.
- (32) Motteler, F. C.; Dash, J. G. *Phys. Rev. B* **1985**, *31*, 346.
- (33) Wiechert, H.; Freimuth, H.; Schildberg, H. P.; Lauter, H. J. *Jpn. J. Appl. Phys.* **1987**, *26* (Suppl. 26-3), 351.
- (34) Schildberg, H. P.; Lauter, H. J.; Freimuth, H.; Wiechert, H.; Haensel, R. *Jpn. J. Appl. Phys.* **1987**, *26* (Suppl. 26-3), 345.
- (35) Cui, J.; Fain, S. *Bull. Am. Phys. Soc.* **1986**, *31*, 376; *J. Vac. Sci. Technol. A* **1987**, *5*, 710; *Bull. Am. Phys. Soc.* **1987**, *32*, 466. Cui, J.; Fain, S. C., Jr.; Freimuth, H.; Wiechert, H.; Schildberg, H. P.; Lauter, H. J. *Phys. Rev. Lett.* **1988**, *60*, 1848.
- (36) Cui, J.; Fain, S. C. *Phys. Rev. B* **1989**, *39*, 8628.
- (37) Ni, X. Z.; Bruch, L. W. *Phys. Rev. B* **1986**, *33*, 4584.
- (38) Palmer, R. E.; Willis, R. F. *Surf. Sci.* **1987**, *179*, L1.
- (39) Chen, J. P.; Yang, R. T. *Surf. Sci.* **1989**, *216*, 481.
- (40) Brown, S. M. D.; Dresselhaus, G.; Dresselhaus, M. S. In *Recent Advances in Catalytic Materials*, Symposium Proceedings, Boston, MA, December 2-4, 1997; Rodriguez, N. M., Soled, S. L., Hrbek, J., Eds.; Materials Research Society: Warrendale, PA, 1998; Vol. 473, p 157.
- (41) Klose, S. *Astron. Astrophys.* **1992**, *260*, 321.
- (42) Diehl, L. M. A.; Chaves, F. A. B.; Lerner, E. J. *Low Temp. Phys.* **1993**, *92*, 173.
- (43) Ron, M.; Gruen, D.; Mendelson, M.; Sheft, I. J. *Less-Common Met.* **1980**, *74*, 445.
- (44) Ishikawa, H.; Oguro, K.; Kato, A.; Susuki, H.; Ishii, E. *J. Less-Common Met.* **1986**, *120*, 123.
- (45) Bernauer, O. *Int. J. Hydrogen Energy* **1988**, *13*, 181.
- (46) Sandrock, G. D.; Snape, E. U.S. Patent 4,566,281, 1986.
- (47) Miura, K.; Morimoto, T. *Langmuir* **1991**, *7*, 374.
- (48) Ichimura, K.; Sano, M. *J. Vac. Sci. Technol. A* **1992**, *10*, 543.
- (49) Akuzawa, N.; Amari, Y.; Nakajima, T.; Takahashi, Y. *J. Mater. Res.* **1990**, *12*, 2849.
- (50) Enoki, T.; Miyajima, S.; Sano, M.; Inokuchi, H. *J. Mater. Res.* **1990**, *5*, 435.
- (51) Chen, Z.-M.; Pettitt, M. *Phys. Rev. B* **1992**, *42*, 8173.
- (52) Chen, Z.-M.; Karim, O. A.; Pettitt, M. J. *Chem. Phys.* **1988**, *89*, 1042.
- (53) Rodriguez, N. M.; Oh, S. G.; Downs, W. B.; Pattabiraman, P.; Baker, R. T. K. *Rev. Sci. Instrum.* **1990**, *61*, 1863.
- (54) Ye, Y.; Ahn, C. C.; Witham, C.; Fultz, B.; Liu, J.; Rinzler, A. G.; Colbert, D.; Smith, K. A.; Smalley, R. E. *Appl. Phys. Lett.* **1999**, *74* 2307.